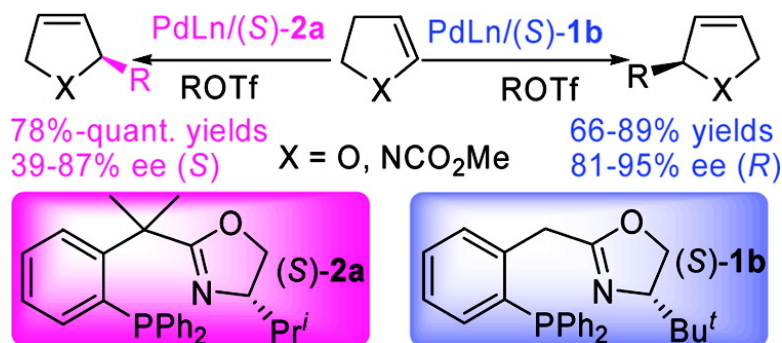


A Dramatic Switch of Enantioselectivity in Asymmetric Heck Reaction by Benzylic Substituents of Ligands

Wen-Qiong Wu, Qian Peng, Da-Xuan Dong, Xue-Long Hou, and Yun-Dong Wu

J. Am. Chem. Soc., **2008**, 130 (30), 9717-9725 • DOI: 10.1021/ja7104174 • Publication Date (Web): 01 July 2008

Downloaded from <http://pubs.acs.org> on February 8, 2009



More About This Article

Additional resources and features associated with this article are available within the HTML version:

- Supporting Information
- Links to the 3 articles that cite this article, as of the time of this article download
- Access to high resolution figures
- Links to articles and content related to this article
- Copyright permission to reproduce figures and/or text from this article

[View the Full Text HTML](#)

A Dramatic Switch of Enantioselectivity in Asymmetric Heck Reaction by Benzylic Substituents of Ligands

Wen-Qiong Wu,[‡] Qian Peng,[‡] Da-Xuan Dong,[†] Xue-Long Hou,^{*,†,‡} and Yun-Dong Wu^{*,‡,§}

State Key Laboratory of Organometallic Chemistry, Shanghai-Hong Kong Joint Laboratory in Chemical Synthesis, Shanghai Institute of Organic Chemistry, Chinese Academy of Sciences, 354 Feng Lin Road, Shanghai, 200032, China, and Department of Chemistry, The Hong Kong University of Science and Technology, Clear Water Bay, Kowloon, Hong Kong, China

Received November 18, 2007; E-mail: xlhou@mail.sioc.ac.cn

Abstract: A series of benzylic substituted *P,N*-ligands **1** and **2** have been synthesized. The Pd-complexes of these ligands show high catalytic activity and enantioselectivity in catalyzing the asymmetric Heck reaction. A dramatic switch in enantioselectivity is realized using ligands with and without substituents at the benzylic position of the ligand. Ligands **1** with H as the substituents offer products in (*R*)-configuration while ligands **2** with the methyl as substituents result in (*S*)-configuration products. In most cases high enantioselectivities are achieved. Density functional theory calculations on the reaction mechanism as well as X-ray analysis of **1a**-PdCl₂ and **2a**-PdCl₂ complexes provide a rational explanation for the above observations.

Introduction

Both enantiomers of a chiral compound may often be demanded in organic synthesis, medicinal and biological chemistry, and the pharmaceutical industry. Usually, they can be obtained by using chiral ligands with opposite configurations in asymmetric catalysis.¹ However, the antipodes of ligands are not always easily available. Thus, many strategies have been developed to realize the tuning of enantioselectivity of reactions² using single ligands with different transition metals,³ solvents,⁴ or temperatures.⁵ There are also some examples of the reversal of enantioselectivity using ligands with a single chiral

backbone simply by modifying some groups of the ligands⁶ or using other approaches.⁷ Recently, an excellent example of a hydrogen-bond-directed reversal of enantioselectivity was also reported.⁸

In the course of studying reaction selectivity control,⁹ we observed that ligands with substituents at the benzylic position showed higher catalytic activities in a Pd-catalyzed asymmetric Heck reaction and an allylic alkylation reaction.¹⁰ Further structural modification of ligands revealed that the substituent

[‡] State Key Laboratory of Organometallic Chemistry.

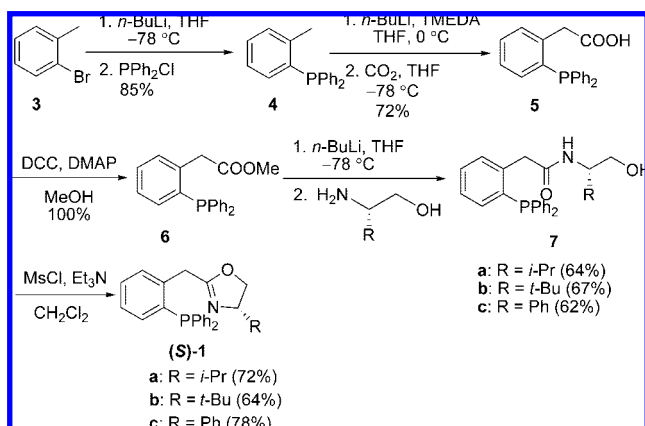
[†] Shanghai-Hong Kong Joint Laboratory in Chemical Synthesis.

[§] The Hong Kong University of Science and Technology.

- (1) Jacobsen, E. N.; Pfaltz, A.; Yamamoto, H., Eds. *Comprehensive Asymmetric Catalysis*; Springer: Heidelberg, 1999.
- (2) For reviews: (a) Sibi, M. P.; Liu, M. *Curr. Org. Chem.* **2001**, *5*, 719. (b) Zanoni, G.; Castronovo, F.; Franzini, M.; Vidari, G.; Giannini, E. *Chem. Soc. Rev.* **2003**, *32*, 115.
- (3) Some examples: (a) Nishibayashi, Y.; Segawa, K.; Takada, H.; Ohe, K.; Uemura, S. *Chem. Commun.* **1996**, 847. (b) Nishibayashi, Y.; Segawa, K.; Ohe, K.; Uemura, S. *Organometallics* **1995**, *14*, 5486. (c) Murakami, M.; Itami, K.; Ito, Y. *J. Am. Chem. Soc.* **1999**, *121*, 4130. (d) Yabu, K.; Masumoto, S.; Yamasaki, S.; Hamashima, Y.; Kanai, M.; Du, W.; Curran, D. P.; Shibasaki, M. *J. Am. Chem. Soc.* **2001**, *123*, 9908. (e) Luna, A. P.; Bonin, M.; Micouin, L.; Husson, H. P. *J. Am. Chem. Soc.* **2002**, *124*, 12098. (f) Du, D. M.; Lu, S. F.; Fang, T.; Xu, J. *J. Org. Chem.* **2005**, *70*, 3712.
- (4) Some examples: (a) Arseniyadis, S.; Valleix, A.; Wagner, A.; Mioskowski, C. *Angew. Chem., Int. Ed.* **2004**, *43*, 3314. (b) Zhou, J.; Tang, Y. *Chem. Commun.* **2004**, 432. (c) Zhou, J.; Ye, M. C.; Huang, Z. Z.; Tang, Y. *J. Org. Chem.* **2004**, *69*, 1309. (d) Thorhauge, J.; Roberson, M.; Hazell, R. G.; Jørgensen, K. A. *Chem.—Eur. J.* **2002**, *8*, 1888. (e) Johannsen, M.; Jørgensen, K. A. *Tetrahedron* **1996**, *52*, 7321. (f) Kanai, M.; Koga, K.; Tomioka, K. *J. Chem. Soc., Chem. Commun.* **1993**, 1248.
- (5) Some examples: (a) Berkessel, A.; Mukherjee, S.; Lex, J. *Synlett* **2006**, 41. (b) Trost, B. M.; Fettes, A.; Shireman, B. T. *J. Am. Chem. Soc.* **2004**, *126*, 2660. (c) Casey, C. P.; Martins, S. C.; Fagan, M. A. *J. Am. Chem. Soc.* **2004**, *126*, 5585. (d) Sibi, M. P.; Gorikunti, U.; Liu, M. *Tetrahedron* **2002**, *58*, 8357.

- (6) (a) Busacca, C. A.; Grossbach, D.; So, R. C.; O'Brien, E. M.; Spinelli, E. M. *Org. Lett.* **2003**, *5*, 595. (b) Busacca, C. A. *J. Org. Chem.* **2004**, *69*, 5187. (c) Hoarau, O.; Ait-Haddou, H.; Daran, J. C.; Cramailère, D.; Balavoine, G. G. A. *Organometallics* **1999**, *18*, 4718. (d) Ait-Haddou, H.; Hoarau, O.; Cramailère, D.; Pezet, F.; Daran, J. C.; Balavoine, G. G. A. *Chem.—Eur. J.* **2004**, *10*, 699. (e) Clyne, D. S.; Mermet-Bouvier, Y. C.; Nomura, N.; RajanBabu, T. V. *J. Org. Chem.* **1999**, *64*, 7601.
- (7) Some examples: (a) Kitagawa, O.; Matsuo, S.; Yotsumoto, K.; Taguchi, T. *J. Org. Chem.* **2006**, *71*, 2524. (b) Lutz, F.; Igarashi, T.; Kawasaki, T.; Soai, K. *J. Am. Chem. Soc.* **2005**, *127*, 12206. (c) Mao, J.; Wan, B.; Zhang, Z.; Wang, R.; Wu, F.; Lu, S. *J. Mol. Catal. A* **2005**, *225*, 33. (d) Danjo, H.; Higuchi, M.; Yada, M.; Imamoto, T. *Tetrahedron Lett.* **2004**, *45*, 603. (e) Kuwano, R.; Sawamura, M.; Ito, Y. *Bull. Chem. Soc. Jpn.* **2000**, *73*, 2571. (f) Evans, D. A.; Kozłowski, M. C.; Murry, J. A.; Burgey, C. S.; Campos, K. R.; Connell, B. T.; Staples, R. J. *J. Am. Chem. Soc.* **1999**, *121*, 669. (g) Ashimori, A.; Overman, L. E. *J. Org. Chem.* **1992**, *57*, 4571.
- (8) Zeng, W.; Chen, G. Y.; Zhou, Y. G.; Li, Y. X. *J. Am. Chem. Soc.* **2007**, *129*, 750.
- (9) (a) Dai, L. X.; Tu, T.; You, S. L.; Deng, W. P.; Hou, X. L. *Acc. Chem. Res.* **2003**, *36*, 659. (b) Zhou, Y. G.; Li, A. H.; Hou, X. L.; Dai, L. X. *Chem. Commun.* **1996**, 1353. (c) Zhou, Y. G.; Li, A. H.; Dai, L. X.; Hou, X. L. *Huaxue Xuebao* **2000**, *58*, 473. (d) You, S. L.; Zhu, X. Z.; Luo, Y. M.; Hou, X. L.; Dai, L. X. *J. Am. Chem. Soc.* **2001**, *123*, 7471. (e) Yang, X. F.; Zhang, M. J.; Hou, X. L.; Dai, L. X. *J. Org. Chem.* **2002**, *67*, 8097. (f) Tu, T.; Deng, W. P.; Hou, X. L.; Dai, L. X.; Dong, X. C. *Chem.—Eur. J.* **2003**, *9*, 3073. (g) Hou, X. L.; Sun, N. *Org. Lett.* **2004**, *6*, 4399. (Corrections: *Org. Lett.* **2005**, *7*, 1435). (h) Zheng, W. H.; Sun, N.; Hou, X. L. *Org. Lett.* **2005**, *7*, 5151. (i) Yan, X. X.; Peng, Q.; Zhang, Y.; Zhang, K.; Hong, W.; Hou, X. L.; Wu, Y. D. *Angew. Chem., Int. Ed.* **2006**, *45*, 1979.

Scheme 1. Synthesis of Ligands 1



at the benzylic position had great impact on the stereoselectivity of the reactions. The configuration of products was switchable when ligands **1** ($R^1 = H$) and **2** ($R^1 = Me$) were used in Pd-catalyzed asymmetric Heck reactions. Here, we report our results on the application of these ligands in Pd-catalyzed asymmetric intermolecular Heck reactions of 2,3-dihydrofuran and *N*-carbomethoxy-2,3-dihydropyrrole as well as a detailed computational study for the rationalization of the observed stereochemistry.^{10d}

Results and Discussion

The preparation of ligands **1** is depicted in Scheme 1. Lithiation of *o*-bromotoluene **3** with *n*-BuLi followed by quenching with PPh₂Cl gave phosphine **4**.¹¹ Direct benzylic-lithiation of **4** and quenching with CO₂ provided acid **5**.¹² Esterification of acid **5** followed by treatment with *n*-BuLi and amino alcohols afforded amides **7**, and ring-closure of **7** gave rise to ligands **1a–c**.

The synthesis of ligands **2** is outlined in Scheme 2. Reaction of compound **8**¹³ with SOCl₂ and then with corresponding amino alcohols provided amides **9**, from which oxazolines **10** were prepared according to the literature procedure.¹⁴ Lithiation of **10** with *n*-BuLi at -78 °C followed by quenching with PPh₂Cl resulted in ligands **2**.

Scheme 2. Synthesis of Ligands 2

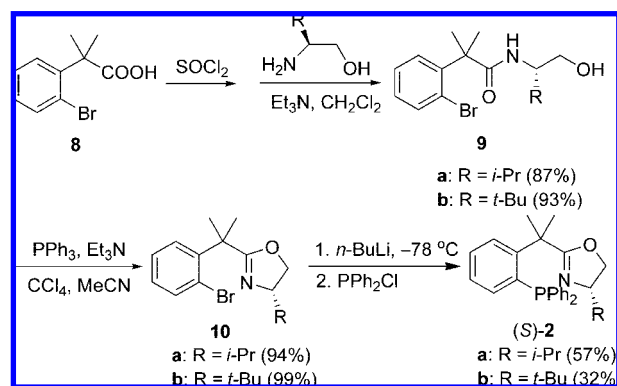
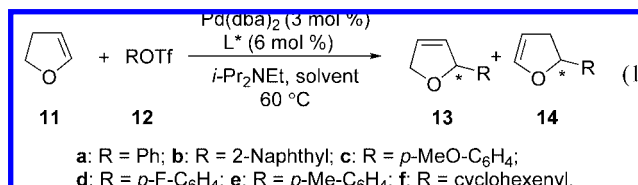


Table 1. Pd-Catalyzed Asymmetric Heck Reaction of **11** Using Ligands **1** and **2**^a

entry	ligand	12	yield, % ^b	13/14 ^c	ee, % (13) ^d
1	1a	12a	62	80/1	78 (<i>R</i>)
2	1b	12a	79	80/1	93 (<i>R</i>)
3	1c	12a	93	50/1	61 (<i>R</i>)
4	2a	12a	86	50/1	81 (<i>S</i>)
5	2b	12a	78	50/1	10 (<i>S</i>)
6	1b	12b	89	18/1	86 (<i>R</i>)
7	2a	12b	quant.	18/1	39 (<i>S</i>)
8	1b	12c	77 ^e	n.d. ^g	82 (<i>R</i>)
9	2a	12c	90 ^f	n.d. ^g	82 (<i>S</i>)
10	1b	12d	66	70/1	87 (<i>R</i>)
11	2a	12d	83	1/0	87 (<i>S</i>)
12	1b	12e	82	100/1	89 (<i>R</i>)
13	2a	12e	78	100/1	84 (<i>S</i>)
14	1b	12f	69	40/1	95 (<i>R</i>)
15	2a	12f	quant.	100/1	65 (<i>S</i>)

^a Reaction conditions: **11** (0.5 mmol), **12** (2 mmol), Pd(dba)₂ (3 mol %), ligand (6 mol %), *i*-Pr₂NEt (1 mol), solvent (2.5 mL, THF for entries 1–5, benzene for entries 6–15). ^b Isolated yields of **13** and **14**. ^c Determined by GC. ^d Determined by GC or HPLC using chiral columns. The absolute configuration of products was assigned according to the reference method.^{9f} ^e Pd(OAc)₂ was used as the palladium source. Isolated yield of **13c** after 40 h. ^f Yield of **13c** and Pd(OAc)₂ was used. ^g Not determined.

With these ligands in hand, we applied them to the Pd-catalyzed asymmetric intermolecular Heck reaction of 2,3-dihydrofuran **11** with aryl triflates **12a–e** and cyclohexenyl triflate **12f** using 3 mol % of Pd(dba)₂ and 6 mol % of ligands with *i*-Pr₂NEt as a base in THF at 60 °C (eq 1).^{15,10c} The results are shown in Table 1.



The ligands appeared to be more active in the intermolecular Heck reaction than other reported ligands did.¹⁵ All the reactions completed in 20 h monitored by TLC, providing 2-substituted-2,5-dihydrofuran **13** predominantly. It is intriguing that **13** was obtained as an (*R*)-enantiomer when ligands **1a–c** were used (entries 1–3, 6, 8, 12, 14), while (*S*)-**13** was afforded when ligands were **2a–b** (entries 4, 5, 7, 9, 11, 13, 15). **1** and **2** have the same configuration. Thus, the dimethyl groups at the

- (10) (a) Hou, X. L.; Wu, X. W.; Dai, L. X.; Cao, B. X.; Sun, J. *Chem. Commun.* **2000**, 1195. (b) Wu, H.; Wu, X. W.; Hou, X. L.; Dai, L. X.; Wang, Q. R. *Chin. J. Chem.* **2002**, *20*, 816. (c) Hou, X. L.; Dong, D. X.; Yuan, K. *Tetrahedron: Asymmetry* **2004**, *15*, 2189. (d) Preliminary results on the application of ligands **1** in Pd-catalyzed asymmetric Heck reaction of 2,3-dihydrofuran have been reported; see ref 10c.
- (11) Tanner, D.; Wyatt, P.; Johansson, F.; Bertilsson, S. K.; Andersson, P. G. *Acta Chem. Scand.* **1999**, *53*, 263.
- (12) Hingst, M.; Tepper, M.; Stelzer, O. *Eur. J. Inorg. Chem.* **1998**, 73.
- (13) Beak, P.; Kerrick, S. T.; Gallagher, D. J. *J. Am. Chem. Soc.* **1993**, *115*, 10628.
- (14) Vorbrüggen, H.; Krolkiewicz, K. *Tetrahedron Lett.* **1981**, *22*, 4471.
- (15) For some recent reviews, see: (a) Tietze, L. T.; Ila, H.; Bell, H. P. *Chem. Rev.* **2004**, *104*, 3453. (b) Shibasaki, M.; Vogl, E. M.; Ohshima, T. *Adv. Synth. Catal.* **2004**, *346*, 1533. (c) Tietze, L. F.; Lotz, F. In *Asymmetric Synthesis*; Christmann, M.; Braese, S., Eds.; Wiley-VCH: Weinheim, 2007, p 147. (d) Shibasaki, M.; Vogl, E. M. In *Comprehensive Asymmetric Catalysis*; Jacobsen, E. N.; Pfaltz, A.; Yamamoto, H., Eds.; Springer: Berlin and Heidelberg, 1999; p 458. For some examples of intermolecular asymmetric Heck reactions: (e) Ozawa, F.; Kubo, A.; Hayashi, T. *J. Am. Chem. Soc.* **1991**, *113*, 1417. (f) Loiseleur, O.; Meier, P.; Pfaltz, A. *Angew. Chem., Int. Ed. Engl.* **1996**, *35*, 200. (g) Tietze, L. F.; Thede, K.; Sannicolò, F. *Chem. Commun.* **1999**, 1811. (h) Yonehara, K.; Mori, K.; Hashizume, T.; Chung, K. G.; Ohe, K.; Uemura, S. *J. Organomet. Chem.* **2000**, *603*, 40. (i) Mata, Y.; Pàmies, O.; Diéguez, M. *Chem.–Eur. J.* **2007**, *13*, 3296.

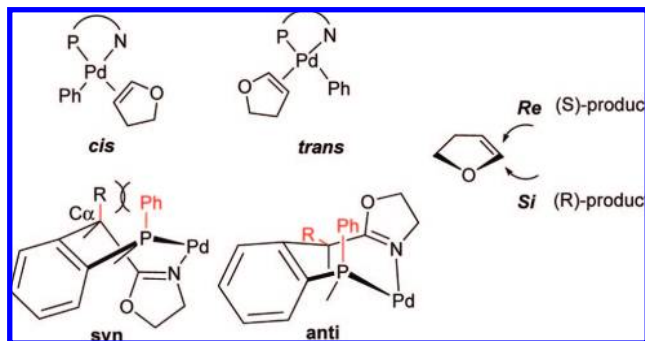
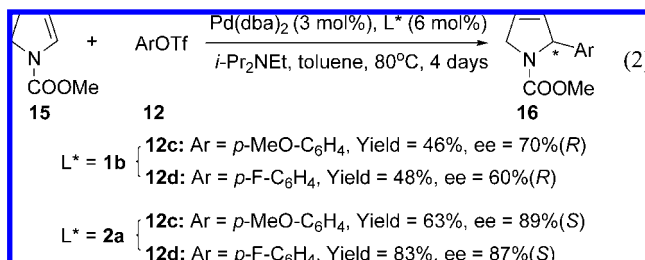


Figure 1. Three modes in the asymmetric phenyl insertion reaction.

benzylic position of the ligand have a significant impact on the stereochemistry of the reactions.¹⁶

The enantioselectivity is also affected by the R group on the oxazoline ring. In the case of ligands **1**, (*R*)-2-phenyl-2,5-dihydrofuran **13a** in 93% ee was obtained when ligand **1b** with a *tert*-butyl group on the oxazoline ring was used while the ee value of **13a** decreased to 78% and 61% if **1a** and **1c** with an *iso*-propyl and a phenyl group on the oxazoline ring was the ligand, respectively (entry 2 vs entries 1 and 3). For ligands **2** with two methyl groups at the benzylic position, better ee of (*S*)-**13a** was obtained by using ligand **2a** with *iso*-propyl as the substituent on the oxazoline ring than by using **2b** with *tert*-butyl as the substituent (entry 4 vs entry 5). It is interesting that higher enantioselectivity is obtained with more bulky R² for ligands **1** while it is the opposite for ligands **2**.

In order to verify further the reversal of the enantioselectivity using these ligands, Heck reactions of *N*-carbomethoxy-2,3-dihydropyrrole **15** with some aryl triflates were carried out (eq 2).^{17,18} Still, ligand **1b** yielded products **16** as (*R*)-enantiomers while ligand **2a** led to (*S*)-enantiomers. Ligand **2a** demonstrated better activities than ligand **1b** did.



To reveal the effect of the geminal dimethyl groups at the benzylic position of the ligand and rationalize the reversal of the enantioselectivity, density functional theory (DFT) calculations were used to model the asymmetric insertion step of the Heck reaction (Scheme 3). Three different modes in the asymmetric insertion need to be studied, as shown in Figure 1.

(16) There have been many examples of geminal alkyl group effect on reactivity and stereochemistry. For reviews, see: Jung, M. E.; Piizzi, G. *Chem. Rev.* **2005**, *105*, 1735.

(17) (a) Ozawa, F.; Hayashi, T. *J. Organomet. Chem.* **1992**, *428*, 267. (b) Tietze, L. F.; Thede, K. *Synlett* **2000**, 1470. (c) Loiseleur, O.; Hayashi, M.; Schmees, N.; Pfaltz, A. *Synthesis* **1997**, 1338. (d) Tu, T.; Hou, X. L.; Dai, L. X. *Org. Lett.* **2003**, *5*, 3651.

(18) The reaction was carried out with a 0.5 mmol scale (**12/15** = 1/4) in the presence of Pd(*dba*)₂ (3 mol %) and the ligand (6 mol %) with *i*-Pr₂NEt (200 mol %) as a base in 2.5 mL of toluene under an argon atmosphere for 4 days. The ee value of **16** was determined by chiral HPLC. Absolute configuration of products was assigned according to ref 17a.

That is, (1) the coordination of dihydrofuran can be either *cis* or *trans* with respect to ligand oxazoline N; (2) the seven-membered ring formed by the ligand coordination with Pd can be in either the *syn* or *anti* conformation according to the orientation of the benzylic substituents and the phenyl group on phosphorus; (3) the addition of Ph can be on either the *Re* or *Si* face of dihydrofuran. Overall, eight transition states are possible. Six of the possible transition states for the reactions of **1a**-Pd and **2a**-Pd with 2,3-dihydrofuran **11** were fully optimized with the density functional theory method of B3LYP/6-31G*(Lan12DZ for Pd and P).¹⁹ The relative energies and some selected bond lengths of the six transition states along with those of the corresponding precursor complexes (**CP2**) are given in Table 2. The other two possible transition states, *cis-anti-Si* and *cis-anti-Re*, were not calculated because of expected high instabilities (see below).

Trans versus Cis. The calculations indicate that, for complex **CP2**, the *cis* mode is apparently more stable than the *trans* mode, but the *trans* mode of the transition states (**TS1**) is much more stable than the *cis* mode with both ligands **1a** and **2a**. These results can be rationalized by ligand–ligand interactions. **CP2** and **TS1** structures are all in a square-planar geometry.^{20,21} As shown in Figure 2, the dihydrofuran coordinates to Pd in a perpendicular geometry to facilitate a π -back-donation. Since P is a more powerful σ -donor and π -acceptor than N,²² it has a larger *trans*-influence. That is, the bond *anti* to P is more weakened. This is clearly indicated by the calculated bond distances as shown in Table 2 and in Figure 2: the Pd(1)–C(2) distance is 2.010 Å in the *cis-syn-Re* structure and is increased to 2.019 Å in the *trans-syn-Re* structure, which is the main cause of destabilization for the *trans-syn-Re* structure. This effect is

(19) The calculations were performed with Gaussian 03 program: Frisch, M. J. et al. *Gaussian 03*, revision C.02; Gaussian, Inc.: Wallingford, CT, 2004.

(20) For selected papers on the calculation of Heck reaction, see: (a) Dotta, P.; Magistrato, A.; Rothlisberger, U.; Pregosin, P. S.; Albinati, A. *Organometallics* **2002**, *21*, 3033. (b) von Schenck, H.; Åkermark, B.; Svensson, M. *J. Am. Chem. Soc.* **2003**, *125*, 3503. (c) Deeth, R. J.; Smith, A.; Brown, J. M. *J. Am. Chem. Soc.* **2004**, *126*, 7144. (d) Lin, B. L.; Liu, L.; Fu, Y.; Luo, S. W.; Chen, Q.; Guo, Q. X. *Organometallics* **2004**, *23*, 2114. (e) Mota, A. J.; Dedieu, A.; Bour, C.; Suffert, J. *J. Am. Chem. Soc.* **2005**, *127*, 7171. (f) Tabares-Mendoza, C.; Guadarrama, P. *J. Organomet. Chem.* **2006**, *691*, 2978. (g) Cui, X.; Li, Z.; Tao, C. Z.; Xu, Y.; Li, J.; Liu, L.; Guo, Q. X. *Org. Lett.* **2006**, *8*, 2467. (h) Datta, G. K.; von Schenck, H.; Hallberg, A.; Larhed, M. *J. Org. Chem.* **2006**, *71*, 3896. (i) Lee, M. T.; Lee, H. M.; Hu, C. H. *Organometallics* **2007**, *26*, 1317.

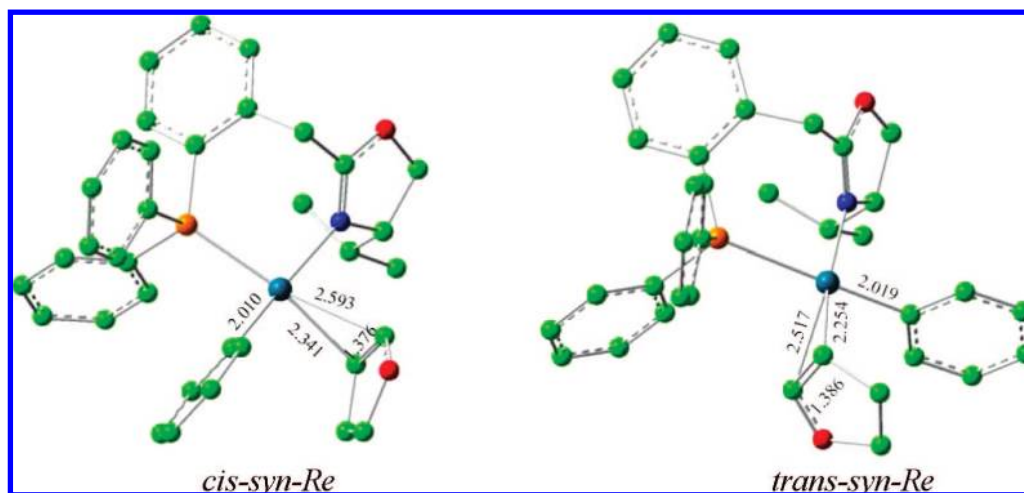
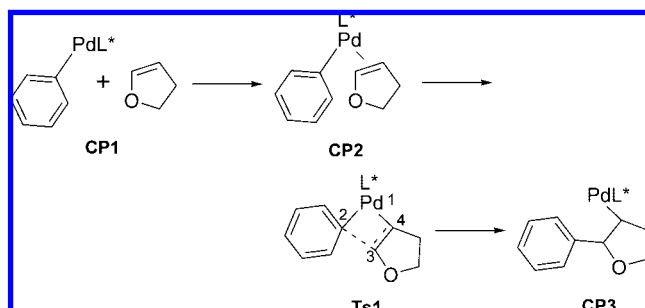
(21) For selected papers on the calculation of oxidative addition: (a) Goossen, L. J.; Koley, D.; Hermann, H. L.; Thiel, W. *Chem. Commun.* **2004**, 2141. (b) Goossen, L. J.; Koley, D.; Hermann, H. L.; Thiel, W. *Organometallics* **2005**, *24*, 2398. (c) Goossen, L. J.; Koley, D.; Hermann, H. L.; Thiel, W. *J. Am. Chem. Soc.* **2005**, *127*, 11102. (d) Fazaeli, R.; Ariaifard, A.; Jamshidi, S.; Tabatabaie, E. S.; Pishro, K. A. *J. Organomet. Chem.* **2007**, *692*, 3984. (e) Fairlamb, I. J. S.; Lee, A. F. *Organometallics* **2007**, *26*, 4087. (f) Lam, K. C.; Marder, T. B.; Lin, Z. Y. *Organometallics* **2007**, *26*, 758. (g) Kozuch, S.; Amatore, C.; Jutand, A.; Shaik, S. *Organometallics* **2005**, *24*, 2319. (h) Ariaifard, A.; Lin, Z. Y. *Organometallics* **2006**, *25*, 4030.

(22) For selected papers, see: (a) Goldfuss, B. *J. Organomet. Chem.* **2006**, 4508. (b) Goldfuss, B.; Löschnann, T.; Rominger, F. *Chem.–Eur. J.* **2004**, *10*, 5422. (c) Tu, T.; Zhou, Y. G.; Hou, X. L.; Dai, L. X.; Dong, X. C.; Yu, Y. H.; Sun, J. *Organometallics* **2003**, *22*, 1255. (d) Kollmar, M.; Steinhagen, H.; Janssen, J. P.; Goldfuss, B.; Malinovsky, S. A.; Vázquez, J.; Rominger, F.; Helmchen, G. *Chem.–Eur. J.* **2002**, *8*, 3103. (e) Steinhagen, H.; Reggelin, M.; Helmchen, G. *Angew. Chem., Int. Ed. Engl.* **1997**, *36*, 2108. (f) Togni, A.; Burckhardt, U.; Gramlich, V.; Pregosin, P. S.; Salzmann, R. *J. Am. Chem. Soc.* **1996**, *118*, 1031. (g) Lin, Z. Y.; Hall, M. B. *Inorg. Chem.* **1991**, *30*, 646. (h) Keith, J. A.; Behenna, D. C.; Mohr, J. T.; Ma, S.; Marinescu, S. C.; Oxgaard, J.; Stoltz, B. M.; Goddard, W. A., III. *J. Am. Chem. Soc.* **2007**, *129*, 11876.

Table 2. Selected Bond Lengths (Å) and Relative Free Energies (kcal/mol) of Calculated Complexes and Transition States in the Insertion Reaction Step (Scheme 3)^a

structure	1a								2a							
	CP2				TS1				CP2				TS1			
	Pd1–C2	$\Delta G_{333K}^{\text{g/s}}$	$\Delta G_{333K}^{\text{g/s}}$	Pd1–C2	C2–C3	$\Delta G_{333K}^{\text{g/s}}$	$\Delta G_{333K}^{\text{g/s}}$	Pd1–C2	$\Delta G_{333K}^{\text{g/s}}$	$\Delta G_{333K}^{\text{g/s}}$	Pd1–C2	C2–C3	$\Delta G_{333K}^{\text{g/s}}$	$\Delta G_{333K}^{\text{g/s}}$		
<i>cis-syn-Si</i>	2.010	-2.5/-3.6	-2.7/-3.7	2.158	2.027	3.6/2.5	3.9/2.8	2.011	0.1/-1.7	-0.2/-2.1	2.160	2.029	5.2/4.1	5.3/3.8		
<i>cis-syn-Re</i>	2.010	-2.8/-4.6	-2.9/-4.6	2.160	2.006	6.3/5.1	6.7/5.7	2.010	0.2/-1.8	-0.1/-2.1	2.162	2.000	8.3/6.2	8.6/6.7		
<i>trans-syn-Si</i>	2.021	0.0/0.0	0.0/0.0	2.152	2.127	0.0/0.0	0.0/0.0	2.022	2.7/1.9	2.5/1.7	2.156	2.131	1.9/1.6	1.6/1.2		
<i>trans-syn-Re</i>	2.019	-0.5/-0.9	-0.2/-0.6	2.146	2.124	0.7/0.5	0.9/0.7	2.023	1.9/1.0	2.0/1.1	2.150	2.125	2.8/1.9	2.9/1.9		
<i>trans-anti-Si</i>	2.016	0.7/-0.1	0.8/0.0	2.147	2.124	2.5/2.0	2.6/2.0	2.019	-0.5/-0.5	-0.3/-0.3	2.147	2.117	0.8/0.6	1.0/0.7		
<i>trans-anti-Re</i>	2.014	0.8/-0.4	0.7/-0.5	2.147	2.137	1.8/1.6	1.8/1.2	2.019	0.0/0.0	0.0/0.0	2.149	2.134	0.0/0.0	0.0/0.0		

^a g/s: the gas phase/with solvation effects; G_{333K} : relative free energies with 6-31G. G'_{333K} : relative free energies with single-point energies (6-311+G** basis set for H, C, N, and O) and frequency calculation with the 6-31G* basis set for H, C, N, and O).

**Figure 2.** Calculated complex structures (CP2 in Scheme 3) mediated by Pd-1a. For clarity, most hydrogen atoms are omitted.**Scheme 3.** Asymmetric Insertion Step of the Heck Reaction

transferred to the transition state as the *trans*-effect; that is, the Pd–Ph bond is more activated in the *trans* mode, and it is more reactive toward the C–C coupling reaction. In addition, the C=C bond in the *trans-syn-Re* is better activated as indicated by its longer C(3)–C(4) bond length (1.386 Å) than that in the *cis-syn-Re* structure (1.376 Å). Therefore, the *trans*-Ph group can proceed with the addition to the 2,3-dihydrofuran double bond with an earlier transition state (longer forming C(2)–C(3) bond distance and shorter Pd(1)–C(2) bond distance) and a lower activation energy (see Table 2).

Another possibility for the higher reactivity of the *trans* mode might be that it takes less energy to rotate the C=C double bond from the perpendicular conformation in CP2 to a coplanar conformation, which is required for the transition state. Indeed, we were able to locate the coplanar complexes. As given in Supporting Information (Table S2), these structures are all about 4 kcal/mol with respect to their corresponding perpendicular

structures, and there is not a big difference in the rotation energy between the *trans* and the *cis* modes of coordination. Therefore, it cannot be a major factor for the higher reactivity of the *trans* mode.

Syn versus Anti. When ligand **1a** or **2a** coordinates with Pd, two conformations (*syn* and *anti*) are possible for the seven-membered-ring. If we use the plane of the bridging benzene ring as a reference, both the P–Pd and C_α–C(oxazoline) bonds have to be out of the plane. If the P–Pd is below the plane, the C_α–C(oxazoline) bond can be either below or above the plane to form *syn* and *anti* conformations, respectively. The two phenyl groups on P arrange in axial (above the plane) and equatorial (below the plane) positions, respectively. Calculations indicate that the *syn* conformation is more stable than the *anti* (by 1–2 kcal/mol, Table 2) both in the CP2 and in the TS1 with ligand **1a**. The *anti* conformation is less stable because of a larger ring strain. The Pd–N=C(oxazoline)–C_α dihedral angle is about 10°–13° in the *syn* structures, but it is about 33°–36° in the *anti* structures. As a result, the N–Pd binding is stronger in the *syn* than in the *anti* structures, as indicated by the calculated Pd–N distances (~2.210 Å in *syn* and ~2.260 Å in *anti*). On the other hand, ligand **2a** with two methyl groups at the benzylic position favors forming the *anti*-conformation of CP2 and TS1 (by 1–2 kcal/mol, Table 2). If the benzylic group is H (**1a**), the *syn* structure does not suffer from the steric interaction between the benzylic group H and the axial phenyl group on the phosphine; the shortest H–H distance is 2.795 Å. However, when the benzylic groups are methyl, the *syn*

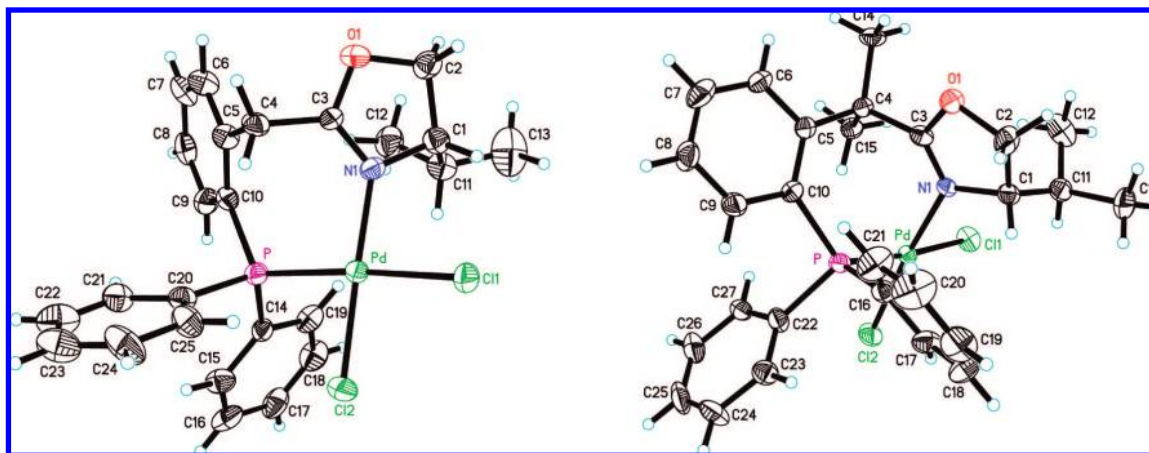


Figure 3. ORTEP drawings of X-ray crystal structures of PdCl₂-**1a** and PdCl₂-**2a** complexes.

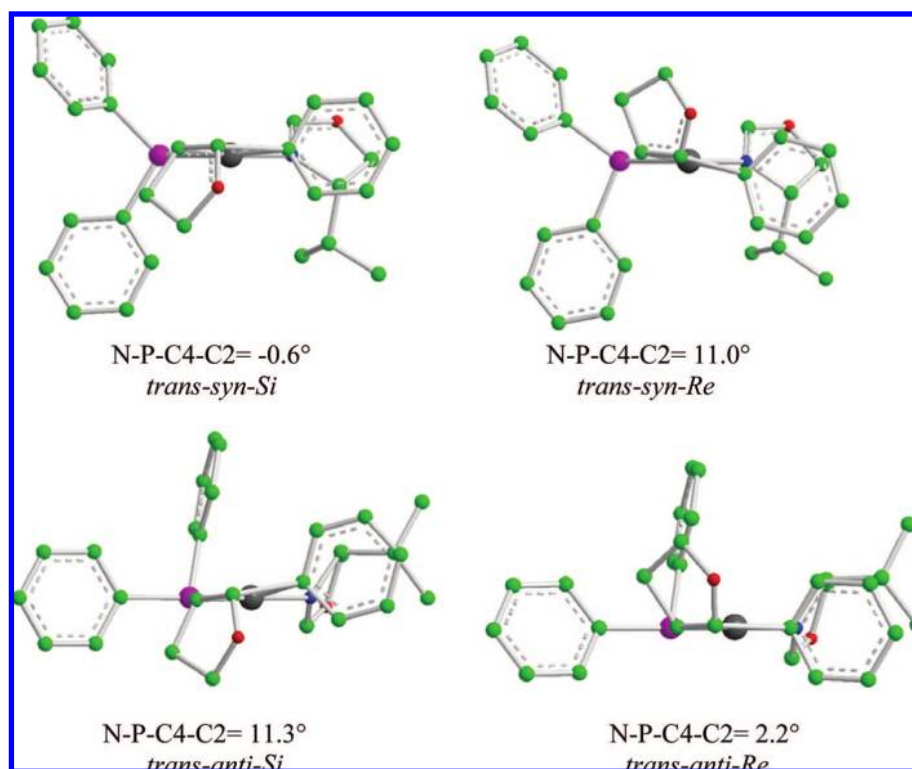


Figure 4. Calculated transition states **TS1** and the dihedral angles for the phenyl insertion reaction step (the number of the atom, see Scheme 3) mediated by Pd-**1a**, in which the phenyl group is *trans* to the P ligand. For clarity, the bridging benzyl group of the ligand and most hydrogen atoms are omitted.

conformation suffers from a significant steric interaction between the axial Me and axial Ph groups, as indicated in Scheme 3.

The above predictions prompted us to obtain crystal structures of the complexes of PdCl₂ with ligands **1a** and **2a**. As shown in Figure 3, X-ray analyses of the two complexes indeed indicate that PdCl₂-**1a** is in a *syn* conformation and PdCl₂-**2a** is in an *anti* conformation.

Re versus Si. As shown in Table 2, no matter whether the ligand is **1a** or **2a**, the *trans-syn-Si* transition state is more stable than the *trans-syn-Re* transition state by 0.7–0.9 kcal/mol. On the other hand, the *trans-anti-Si* transition state is less stable than the *trans-anti-Re* transition state by 0.7–1.0 kcal/mol. Since *trans-syn* is more stable than *trans-anti* for ligand **1a**, the (*R*)-product is predicted to be the major product when the ligand is **1a**. In contrast, *trans-anti* is more stable than *trans-syn* for ligand **2a**, and the (*S*)-product is predicted to be the major product

when the ligand is **2a**. These predictions are in qualitative agreement with experimental observations (Table 1).

Figure 4 shows the four phenyl insertion transition states (**TS1** in Scheme 3) of Pd-**1a**-(phenyl)(2,3-dihydrofuran) with the bridging benzyl group of the ligand deleted for clarity. In these structures, the phenyl group is *trans* to the P atom of the **1a** ligand. The structures are arranged in such a way that P–Pd–N is in the plane perpendicular to the paper. The two favorable transition structures for the *syn* and *anti* conformations, *trans-syn-Si* and *trans-anti-Re*, have a nearly perfect square-planar Pd center (the dihedral angles of N–P–C4–C2 are nearly 0°, Figure 4). On the other hand, the two less favorable transition structures, *trans-syn-Re* and *trans-anti-Si*, have the Pd center distorted away from a square-planar geometry. This situation is exactly the same for the corresponding four transition

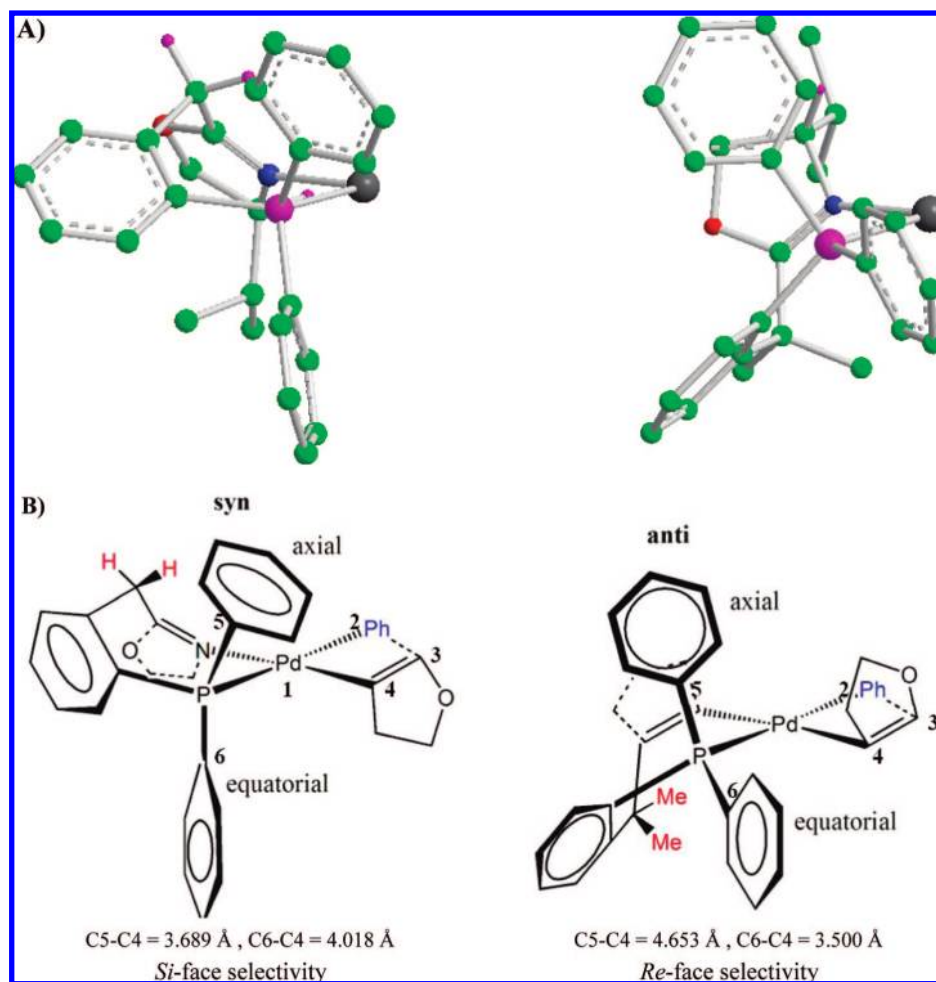


Figure 5. Side view of the *syn* conformation of Pd-**1a** and the *anti* conformation of Pd-**2a** and schematic models for the prediction of enantioselectivity with the two ligands **1a** and **2a**.

structures with **2a** as ligand (see Supporting Information, coordinates of calculated structures in Table S1).

A closer inspection of the transition structures indicates that the distortions in *trans-syn-Re* and *trans-anti-Si* are not caused by the steric interaction between the Pd-bound phenyl group and the oxazoline. The only close contact is between the hydrogen of the isopropyl group and the phenyl group. However, the steric interaction should be about the same for *Si* and *Re* structures without the distortion. Figure 5 shows the side view of the *syn* conformation of Pd-**1a** and the *anti* conformation of Pd-**2a**. Due to the constraint of the seven-membered-ring, the two phenyl groups on P atom create an unsymmetrical environment around the Pd metal center. As shown more clearly by ChemDraw schematic pictures (Figure 5B), in the *syn* conformation, the axial phenyl group is closer to the Pd center (the bond length of C5–C4 is shorter than the one of C6–C4). Thus, it is more crowded above the square-planar Pd plane and less crowded below the Pd plane in the *syn* transition state. On the other hand, in the *anti* conformation, the equatorial phenyl group is closer to the Pd center (the bond length of C6–C4 is shorter) and causes more steric crowding below the Pd plane in the *anti* transition state. This explains why the *trans-syn-Si* and *trans-anti-Re* transition states, which do not need distortion, are more favorable than the *trans-syn-Re* and *trans-anti-Si* transition states, which have to be distorted, respectively. As expected, differences in steric interaction in the products should be even more significant. This is indeed the case. The calculated

preference for the products of *trans-syn-Si* and *trans-anti-Re* over the products of *trans-syn-Re* and *trans-anti-Si* is about 2.4 and 1.8 kcal/mol, respectively (Figure 6, CP3).

The above results also allow us to rationalize the opposite effect of *t*-Bu of ligands **1b** and **2b** on the enantioselectivity that is observed experimentally (Table 1). Both ligands **1a** and **1b** should favor the *syn* conformation. Because of the geometrical distortion in the *trans-syn-Re*, the replacement of the *i*-Pr group by the *t*-Bu group causes more steric interaction to the *trans-syn-Re* than to the *trans-syn-Si*, resulting in increased enantioselectivity. On the other hand, both ligands **2a** and **2b** favor the *anti* conformation. The replacement of the *i*-Pr by the *t*-Bu group introduces more steric interaction to the *trans-anti-Re* than to the *trans-anti-Si*, resulting in decreased enantioselectivity. These qualitative analyses are supported by calculation results. With ligand **2b**, the *trans-anti-Si* transition state is less stable than the *trans-anti-Re* transition state by only 0.4 kcal/mol. The *trans-syn-Si* transition state is much more stable than the *trans-syn-Re* transition state by 1.9 kcal/mol when ligand **1b** is used.

Summary

A series of benzylic substituted *P,N*-ligands **1** and **2** with H and Me as substituents at the benzylic position, respectively, have been synthesized. The palladium complexes of these ligands show high catalytic activity and enantioselectivity in catalyzing the asymmetric Heck reaction. A dramatic switch in

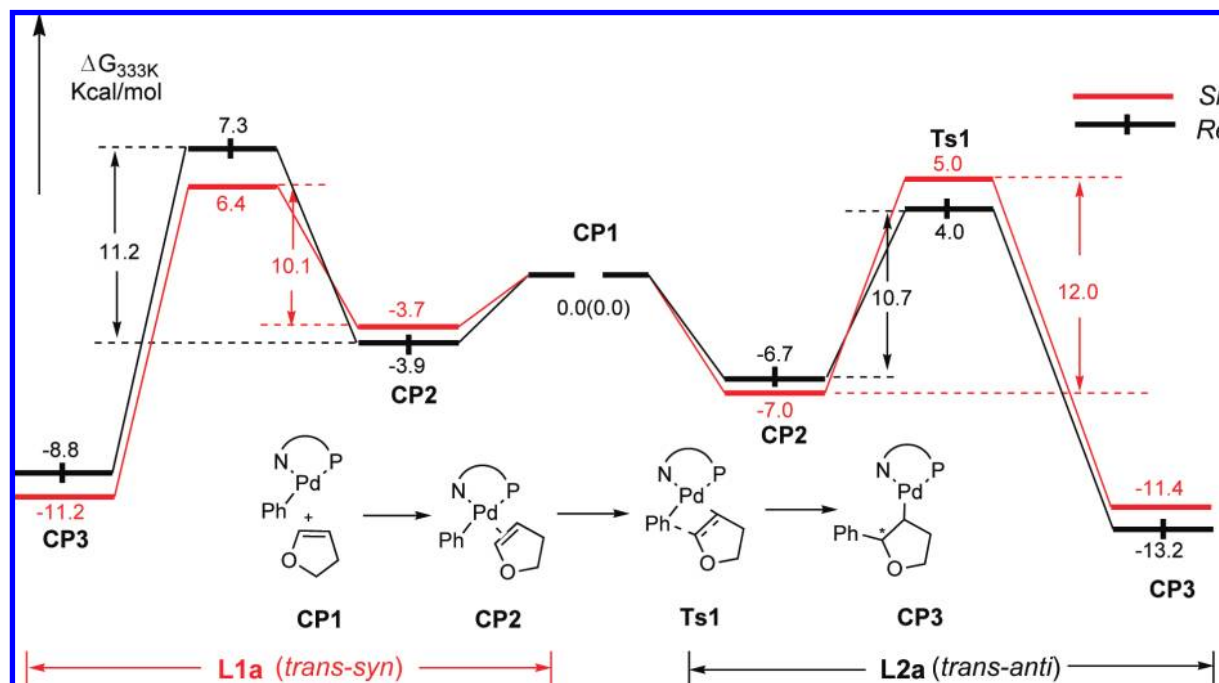


Figure 6. Calculated free energy ($\Delta G'_{333K}$, 6-311+G**) profiles relevant to the *Re*-attack and *Si*-attack in the insertion reaction.

enantioselectivity is realized using ligands with and without substituents at the benzylic position of the ligands. Ligands **1** with $R^1 = H$ offer products in the (*R*)-configuration while ligands **2** with $R^1 = Me$ result in (*S*)-configuration products. In most cases high enantioselectivities are achieved. Density functional theory calculations on the reaction mechanism as well as X-ray analysis of $PdCl_2$ -**1a** and $PdCl_2$ -**2a** complexes provide a rational explanation for the above observations: (1) Ligands **1** and **2** coordinate with Pd in *syn* and *anti* seven-membered ring conformations, respectively; (2) due to the stronger *trans* effect of P over N, the Pd-bound phenyl group prefers *trans* to P in the transition state so that it is more activated with a lower barrier for addition to Pd-coordinated 2,3-dihydrofuran substrate; (3) because of the unsymmetrical environment caused by the two phenyl groups on P (Figure 5), the *trans-syn-Si* and the *trans-anti-Re* transition states are more favorable than *trans-syn-Re* and *trans-anti-Si* transition states, respectively, which require a geometrical distortion away from the square-planar Pd center. Further applications of these ligands in asymmetric catalysis are in progress.

Experimental Section

General Information. All reactions were performed under a dry argon atmosphere. The commercially available reagents were used without further purification. The solvents were treated by using standard methods. Unless otherwise stated, all 1H NMR spectra were recorded in $CDCl_3$ and the chemical shifts were referenced to $CHCl_3$ ($\delta = 7.27$ ppm) or TMS ($\delta = 0$ ppm). The chemical shifts for ^{13}C NMR spectra were referenced to $CDCl_3$ ($\delta = 77.0$ ppm). The chemical shifts for ^{31}P NMR spectra were referenced

to external 85% H_3PO_4 . Optical rotation was measured with a thermally jacketed 10 cm cell at 20 °C (concentration C given as g/100 mL). IR spectra were recorded in KBr and measured in cm^{-1} . Melting points are uncorrected. Diphenyl(*o*-tolyl)phosphine (**4**),¹¹ 2-[2-(diphenylphosphino)phenyl]acetic acid (**5**),¹² and 2-(2-bromophenyl)-2-methylpropanoic acid **8**¹³ were prepared using the literature procedure. Asymmetric Heck reactions proceeded according to the known procedures, and the ee values of products were determined using GC or HPLC with a chiral column.

Preparation of Methyl 2-[2-(diphenylphosphino)phenyl]acetate (6**).** At 0 °C, **5** (4.363 g, 13.6 mmol), DCC (3.330 g, 16.0 mmol), and DMAP (60 mg) were mixed in MeOH (6 mL). The mixture was stirred at room temperature until the reaction was completed monitored by TLC. The reaction mixture was filtered through a silica gel pad and washed with CH_2Cl_2 . After removal of the solvent, the residue was purified by flash chromatography on silica gel (petroleum ether/ethyl acetate = 20) to afford **6** as a white solid (4.586 g, 13.6 mmol, quant.). Mp: 66–68 °C; IR (KBr, cm^{-1}): 3058, 1737, 751, 699; 1H NMR (300 MHz, $CDCl_3$): δ 3.43 (s, 3H), 3.96 (s, 2H), 6.91–6.95 (m, 1H), 7.11–7.40 (m, 13H); ^{31}P NMR (121 MHz, $CDCl_3$): δ -14.31; ^{13}C NMR (75 MHz, $CDCl_3$): δ 39.7 (d, $J_{PC} = 23$ Hz), 51.7, 127.4, 128.4 (d, $J_{PC} = 6.8$ Hz), 128.5 (d, $J_{PC} = 20.5$ Hz), 129.1, 130.5 (d, $J_{PC} = 4.6$ Hz), 133.8 (d, $J_{PC} = 19.5$ Hz), 133.9, 136.1 (d, $J_{PC} = 9.2$ Hz), 136.5 (d, $J_{PC} = 12.6$ Hz), 138.9 (d, $J_{PC} = 26.9$ Hz), 171.5; MS (EI) m/z (%): 334 (M^+ , 3.67), 319 (100). Anal. Calcd for $C_{21}H_{19}O_2P$: C, 75.44; H, 5.73. Found: C, 75.46; H, 5.66.

Preparation of (*S*)-2-[2-(Diphenylphosphino)benzyl]-4-*isopropyl*-4,5-dihydrooxazole (1a**).** To a solution of L-valinol (514 mg, 5.0 mmol) in THF (40 mL) was added *n*-BuLi (1.6 M in hexane, 6.3 mL, 10.0 mmol) dropwise within 20 min at 0 °C. After the mixture was stirred at room temperature for 1 h, a solution of **6** (1.670 g, 5.0 mmol) in THF (10 mL) was added. The reaction mixture was refluxed for 27 h. The reaction mixture was cooled to room temperature, and 20 mL of saturated NH_4Cl aqua solution were added. The organic phase was separated, and the water phase was extracted with EtOAc (20 mL \times 3). The combined organic phases were dried over Na_2SO_4 . After evaporation of the organic solvents, the mixture was purified by flash chromatography on silica gel (petroleum ether/ethyl acetate = 2) to give **7a** as a white solid (1.306 g, 3.2 mmol, 64%).

(23) Yuan, K.; Zhang, T. K.; Hou, X. L. *J. Org. Chem.* **2005**, *70*, 6085.

(24) (a) Becke, A. D. *Phys. Rev.* **1988**, *A38*, 3098. (b) Becke, A. D. *J. Chem. Phys.* **1993**, *98*, 1372. (c) Lee, C.; Yang, W.; Parr, R. G. *Phys. Rev.* **1988**, *B37*, 785.

(25) Wadt, W. R.; Hay, P. J. *J. Chem. Phys.* **1985**, *82*, 284.

(26) (a) Cancès, M. T.; Mennucci, B.; Tomasi, J. *J. Chem. Phys.* **1997**, *107*, 3032. (b) Mennucci, B.; Tomasi, J. *J. Chem. Phys.* **1997**, *106*, 5151. (c) Cossi, M.; Scalmani, G.; Rega, N.; Barone, V. *J. Chem. Phys.* **2002**, *117*, 43.

MsCl (160 mg, 1.40 mmol) was added dropwise over 10 min into a solution of **7a** (567 mg, 1.4 mmol) and Et₃N (1 mL, 7.0 mmol) in CH₂Cl₂ (7 mL) at 0 °C. The reaction mixture was warmed to room temperature and stirred overnight and quenched with H₂O (7 mL). Usual workup gave **1a** as a colorless oil (389 mg, 1.0 mmol, 72%). [α]_D²⁰ –36.0 (c 0.56, CHCl₃); IR (KBr, cm⁻¹): 2960, 2873, 1699, 1435, 745, 697; ¹H NMR (300 MHz, CDCl₃): δ 0.82 (d, *J* = 6.6 Hz, 3H), 0.91 (d, *J* = 6.6 Hz, 3H), 1.59–1.71 (m, 1H), 3.69–3.82 (m, 2H), 3.88–4.05 (m, 3H), 6.88–6.92 (m, 1H), 7.14–7.38 (m, 13H); ³¹P NMR (121 MHz, CDCl₃): δ –14.44; ¹³C NMR (75 MHz, CDCl₃): δ 17.9, 18.8, 32.2, 33.1 (d, *J*_{PC} = 23 Hz), 69.8, 71.8, 127.0, 128.26 (d, *J*_{PC} = 6.8 Hz), 128.32 (d, *J*_{PC} = 16.6 Hz), 128.9, 129.3 (d, *J*_{PC} = 4.6 Hz), 133.63 (d, *J*_{PC} = 20.0 Hz), 133.65 (d, *J*_{PC} = 19.4 Hz), 133.72, 136.1 (d, *J*_{PC} = 13.1 Hz), 136.2 (d, *J*_{PC} = 10.3 Hz), 140.0 (d, *J*_{PC} = 26.8 Hz), 165.1; MS (EI) *m/z* (%): 387 (M⁺, 2.33), 344 (2.25), 316 (100). Anal. Calcd for C₂₅H₂₆NOP: C, 77.50; H, 6.76; N, 3.62. Found: C, 77.38; H, 6.80; N, 3.52.

Preparation of (S)-2-[2-(Diphenylphosphino)benzyl]-4-tert-butyl-4,5-dihydrooxazole (1b). **1b** was prepared as a white solid (43%, two steps) using the same procedure as that for **1a**. Mp: 49–51 °C; [α]_D²⁰ –37.2 (c 1.00, CHCl₃); IR (KBr, cm⁻¹): 2960, 1666, 1471, 1433, 744, 695; ¹H NMR (300 MHz, CDCl₃): δ 0.85 (s, 9H), 3.69–3.76 (m, 1H), 3.87–4.02 (m, 4H), 6.87–6.92 (m, 1H), 7.12–7.40 (m, 13H); ³¹P NMR (121 MHz, CDCl₃): δ –14.36; ¹³C NMR (75 MHz, CDCl₃): δ 25.5, 32.8 (d, *J*_{PC} = 24 Hz), 33.1, 68.2, 75.2, 126.8, 128.13 (d, *J*_{PC} = 6.9 Hz), 128.15 (d, *J*_{PC} = 6.8 Hz), 128.2 (d, *J*_{PC} = 17.2 Hz), 128.7, 129.0 (d, *J*_{PC} = 4.6 Hz), 133.48 (d, *J*_{PC} = 19.4 Hz), 133.52, 135.9 (d, *J*_{PC} = 13.2 Hz), 136.0 (d, *J*_{PC} = 10.3 Hz), 136.1 (d, *J*_{PC} = 10.3 Hz), 139.8 (d, *J*_{PC} = 26.4 Hz), 165.0 (d, *J*_{PC} = 1.2 Hz); MS (EI) *m/z* (%): 401 (M⁺, 6.86), 316 (100). Anal. Calcd for C₂₆H₂₈NOP: C, 77.78; H, 7.03; N, 3.49. Found: C, 77.45; H, 7.05; N, 3.28.

Preparation of (S)-2-[2-(Diphenylphosphino)benzyl]-4-phenyl-4,5-dihydrooxazole (1c). **1c** was prepared as a white solid (48%, two steps) using the same procedure as that for **1a**. Mp: 109–111 °C; [α]_D²⁰ –43.0 (c 1.15, CHCl₃); IR (KBr, cm⁻¹): 1662, 1432, 989, 752, 745, 698; ¹H NMR (300 MHz, CDCl₃): δ 3.90–3.98 (m, 1H), 4.05 (dd, *J* = 15.5, 24 Hz, 2H), 4.36–4.44 (m, 2H), 6.91–6.96 (m, 1H), 7.16–7.48 (m, 18H); ³¹P NMR (121 MHz, CDCl₃): δ –14.44; ¹³C NMR (75 MHz, CDCl₃): δ 33.2 (d, *J*_{PC} = 22.9 Hz), 69.5, 74.6, 126.6, 127.27, 127.34, 128.36, 128.46, 128.6, 129.2, 129.8 (d, *J*_{PC} = 4.6 Hz), 133.6, 133.7, 133.89, 133.95, 136.18, 136.24, 136.30, 136.37, 136.44, 139.9 (d, *J*_{PC} = 26.3 Hz), 142.3, 166.8 (observed complexity due to P-C splitting; definitive assignments have not yet been made); MS (ESI) *m/z*: 422 (M + 1⁺). Anal. Calcd for C₂₈H₂₄NOP: C, 79.79; H, 5.74; N, 3.32. Found: C, 79.62; H, 5.74; N, 3.10.

Preparation of (S)-2-(2-Bromophenyl)-N-(1-hydroxy-3-methylbutan-2-yl)-2-methylpropanamide (9a). ²³ 2-(2-Bromophenyl)-2-methylpropanoic acid **8** (983 mg, 4.0 mmol) was added to thionyl chloride (8 mL). The reaction mixture was refluxed for 3 h, and the excess SOCl₂ was removed in vacuo. Dry CH₂Cl₂ (2 mL) was then added, and the mixture was concentrated in vacuo to remove any remaining SOCl₂ and this was repeated three times. Dry CH₂Cl₂ (8 mL) was then added to the acid chloride. Under an argon atmosphere, L-valinol (500 mg, 4.8 mmol) and Et₃N (0.9 mL, 6.4 mmol) were dissolved in dry CH₂Cl₂ (8 mL) and cooled to 0 °C. The above acyl chloride solution was added dropwise over a period of 0.5 h. The reaction mixture was allowed to warm up to room temperature and stirred overnight. The resulting solution was washed with water (10 mL) and dried over Na₂SO₄. The solvent was removed under reduced pressure, and the crude product was purified by flash chromatography on silica gel (petroleum ether/ethyl acetate = 2) to give **9a** as an oil (1.140 g, 3.5 mmol, 87%). ¹H NMR (300 MHz, CDCl₃): δ 0.79 (d, *J* = 6.6 Hz, 3H), 0.87 (d, *J* = 6.6 Hz, 3H), 1.62–1.72 (m, 6H), 1.72–1.82 (m, 1H), 2.76–2.80 (m, 1H), 3.58–3.79 (m, 3H), 5.25–5.27 (br d, 1H),

7.15–7.21 (m, 1H), 7.35–7.41 (m, 1H), 7.51–7.54 (m, 1H), 7.61–7.64 (m, 1H); MS (EI) *m/z* (%): 328 (M + 1⁺, 100).

Preparation of (S)-2-(2-Bromophenyl)-N-(1-hydroxy-3,3-dimethylbutan-2-yl)-2-methylpropanamide (9b). **9b** was prepared as a white solid (93%) using the same procedure as that for **9a**. Mp: 105–107 °C; IR (KBr, cm⁻¹): 3370, 2958, 2866, 1651, 1504, 1437, 767, 757; ¹H NMR (300 MHz, CDCl₃): δ 0.82 (s, 9H), 1.69–1.71 (m, 6H), 2.98–3.02 (m, 1H), 3.50–3.57 (m, 1H), 3.68–3.74 (m, 1H), 3.79–3.87 (m, 1H), 7.16–7.22 (m, 1H), 7.37–7.42 (m, 1H), 7.53–7.56 (m, 1H), 7.62–7.65 (m, 1H); ¹³C NMR (75 MHz, CDCl₃): δ 26.4, 26.8, 26.9, 33.4, 48.8, 60.4, 63.4, 124.0, 127.9, 128.1, 129.0, 135.0, 142.9, 177.8; MS (EI) *m/z* (%): 286 (M⁺–Bu⁺, 21.81), 284 (M⁺–Bu⁺, 23.53), 199 (95.81), 197 (100.00); Anal. Calcd for C₁₆H₂₄BrNO₂: C, 56.15; H, 7.07; N, 4.09. Found: C, 56.30; H, 6.85; N, 3.98.

Preparation of (S)-2-[2-(2-Bromophenyl)propan-2-yl]-4-iso-propyl-4,5-dihydrooxazole (10a). ²³ To a solution of amide **9a** (1.140 g, 3.5 mmol) in MeCN (8 mL) were added PPh₃ (2.911 g, 11.1 mmol), Et₃N (2.33 mL, 16.7 mmol), and CCl₄ (3.22 mL, 33.3 mmol). The reaction mixture was stirred overnight at room temperature. After completion of the reaction (monitored by TLC), water (10 mL) was added and the resulting mixture was extracted with CH₂Cl₂ (10 mL × 3). The combined organic phase was dried over Na₂SO₄. The solvent was removed under reduced pressure, and the crude product was purified by flash chromatography on silica gel (petroleum ether/ethyl acetate = 10) to give **10a** as a colorless oil (1.020 g, 3.3 mmol, 94%). ¹H NMR (300 MHz, CDCl₃): δ 0.88 (d, *J* = 7.0 Hz, 3H), 0.97 (d, *J* = 7.0 Hz, 3H), 1.71–1.72 (m, 6H), 1.80–1.93 (m, 1H), 3.93–4.01 (m, 2H), 4.18–4.27 (m, 1H), 7.07–7.12 (m, 1H), 7.27–7.33 (m, 1H), 7.42–7.46 (m, 1H), 7.55–7.58 (m, 1H); ¹³C NMR (75 MHz, CDCl₃): δ 17.9, 19.1, 27.2, 27.7, 32.3, 42.4, 70.3, 72.0, 123.8, 127.3, 127.4, 128.2, 134.6, 143.6, 171.7.

Preparation of (S)-2-[2-(2-Bromophenyl)propan-2-yl]-4-tert-butyl-4,5-dihydrooxazole (10b). **10b** was prepared as an oil (99%) using the same procedure as that for **10a**. IR (KBr, cm⁻¹): 2976, 2955, 2903, 2869, 1664, 1471, 756; ¹H NMR (300 MHz, CDCl₃): δ 0.92 (s, 9H), 1.72–1.74 (m, 6H), 3.89–3.95 (m, 1H), 4.01–4.07 (m, 1H), 4.15–4.21 (m, 1H), 7.07–7.13 (m, 1H), 7.28–7.33 (m, 1H), 7.42–7.45 (d, *J* = 8.1 Hz, 1H), 7.55–7.58 (d, *J* = 8.1 Hz, 1H); ¹³C NMR (75 MHz, CDCl₃): δ 26.0, 27.2, 28.0, 34.0, 42.5, 69.1, 75.6, 123.7, 127.3, 127.4, 128.2, 134.6, 143.7, 171.7; MS (EI) *m/z* (%): 324 (M⁺, 0.52), 244 (100); 268 (30.85), 266 (32.06). Anal. Calcd for C₁₆H₂₂BrNO: C, 59.27; H, 6.84; N, 4.32. Found: C, 59.30; H, 6.89; N, 4.14.

Preparation of (S)-2-[2-[2-(Diphenylphosphino)phenyl]propan-2-yl]-4-iso-propyl-4,5-dihydrooxazole (2a). To a solution of **10a** (997 mg, 3.2 mmol) in THF (15 mL) at –78 °C was added *n*-BuLi (1.6 M in hexane, 2.3 mL, 3.7 mmol) dropwise over 5 min. The reaction mixture was stirred for 1 h at that temperature, and then PPh₂Cl (0.67 mL, 3.7 mmol) was added dropwise over 5 min to the solution at –78 °C. The reaction mixture was warmed to room temperature, stirred overnight, and quenched with a saturated NH₄Cl solution (15 mL). The water phase was extracted with Et₂O (15 mL × 3). The combined organic phases were dried over Na₂SO₄. Evaporation of the organic solvents gave a residue, which was purified by flash chromatography on silica gel (petroleum ether/ethyl acetate = 10) to give **2a** as a white solid (766 mg, 1.8 mmol, 57%). Mp: 95–97 °C; [α]_D²⁰ –48.5 (c 0.935, CHCl₃); IR (KBr, cm⁻¹): 3051, 2982, 2953, 2873, 1652, 1478, 747, 737, 695; ¹H NMR (300 MHz, CDCl₃): δ 0.76 (d, *J* = 7.0 Hz, 3H), 0.84 (d, *J* = 7.0 Hz, 3H), 1.73–1.79 (m, 1H), 1.77 (s, 3H), 1.84 (s, 3H), 3.60–3.70 (m, 3H), 7.15–7.40 (m, 13H), 7.51–7.55 (m, 1H); ¹³C NMR (75 MHz, CDCl₃): δ 17.4, 19.1, 29.9 (d, *J*_{PC} = 5.7 Hz), 30.1 (d, *J*_{PC} = 7.4 Hz), 31.8, 42.2 (d, *J*_{PC} = 6.9 Hz), 69.4, 71.8, 125.4, 125.5, 126.8, 127.9, 128.0, 128.1, 128.17, 128.24, 129.6, 133.1 (d, *J*_{PC} = 18.9 Hz), 135.6, 135.9, 138.2, 138.3, 138.40, 138.44, 151.4, (d, *J*_{PC} = 26 Hz), 173.0 (observed complexity due to P-C splitting; definitive assignments have not yet been made); ³¹P NMR (121

MHz, CDCl₃): δ -14.52; MS (ESI) m/z : 416 (M + 1⁺); Anal. Calcd for C₂₇H₃₀NOP: C, 78.05; H, 7.28; N, 3.37. Found: C, 77.98; H, 7.34; N, 3.27.

Preparation of (S)-2-{[2-(Diphenylphosphino)phenyl]propan-2-yl}-4-tert-butyl-4,5-dihydrooxazole (2b). **2b** was prepared as a white solid (32%) using the same procedure as that for **2a**. Mp: 124–126 °C; [α]_D²⁰ -44.5 (*c* 0.70, CHCl₃); IR (KBr, cm⁻¹): 3054, 2983, 2947, 2899, 2865, 1657, 1478, 1432, 746, 696; ¹H NMR (300 MHz, CDCl₃): δ 0.80 (s, 9H), 1.76 (s, 3H), 1.87 (s, 3H), 3.43 (dd, *J* = 8.1, 9.9 Hz, 1H), 3.53–3.58 (m, 1H), 3.73–3.78 (m, 1H), 7.13–7.39 (m, 13H), 7.49–7.54 (m, 1H); ¹³C NMR (75 MHz, CDCl₃): δ 25.9, 29.9 (d, *J*_{PC} = 4.6 Hz), 30.3 (d, *J*_{PC} = 8.6 Hz), 33.8, 42.3 (d, *J*_{PC} = 6.9 Hz), 68.4, 75.5, 125.4, 125.5, 126.8, 127.8, 127.97, 128.04, 128.1, 128.2, 129.54, 133.07 (d, *J*_{PC} = 18.3 Hz), 133.12 (d, *J*_{PC} = 18.9 Hz), 135.7, 136.0, 138.1, 138.3, 138.39, 138.42, 138.6, 151.4 (d, *J*_{PC} = 26 Hz), 172.7 (observed complexity due to P-C splitting; definitive assignments have not yet been made); ³¹P NMR (121 MHz, CDCl₃): δ -14.44; MS (ESI) m/z (%): 430 (M+1⁺). Anal. Calcd for C₂₈H₃₂NOP: C, 78.29; H, 7.51; N, 3.26. Found: C, 78.02; H, 7.48; N, 3.09.

General Experimental Procedure of the Asymmetric Heck Reaction. Pd(dba)₂ (8.6 mg, 0.015 mmol), ligand (0.03 mmol), and solvent (2.5 mL) were placed under an argon atmosphere in a Schlenk tube with a magnetic stirring bar. After the mixture stirred for 30 min, phenyl triflate (112 mg, 0.5 mmol) was added, followed by the addition of 2,3-dihydrofuran (0.15 mL, 2 mmol) and *i*-Pr₂NET (0.17 mL, 1 mmol). The mixture was stirred at 60 °C for about 20 h until the reaction was completed monitored by TLC. The reaction mixture was quenched with additional EtOAc (2 mL), and the resulting suspension was filtered through a short silica gel column to removed the palladium black. The solvent was removed under reduced pressure, and the mixture was purified by flash chromatography on silica gel to afford a mixture of **13** and **14** as a colorless oil. The ratio of **13** and **14** was determined by GC. The ee value of **13** was determined by chiral GC or HPLC.^{9f}

Computational Details. All calculations were carried out with the Gaussian 03 program package.¹⁹ Molecular geometries were

fully optimized with the density functional theory method of B3LYP²⁴ without any symmetry constraint. The effective core potentials (ECPs) of Hay and Wadt with a double- ξ basis set (LanL2DZ) were used for Pd and P,²⁵ and the 6-31G* basis set was used for H, C, N, and O. The energies were further estimated using a larger basis set (6-311+G** basis set for H, C, N, and O) by single-point calculations. Solvent effects was estimated by the integral equation formulation of the polarized continuum model (IEFPCM).²⁶ THF was used as solvent with a dielectric constant value of 7.58 and using UAHF (United Atom Hartree–Fock) radii for the respective (Pd, H, C, N, O, P) in the IEFPCM calculations. The nature of the extrema (local minima or transition states) was checked by analytical frequency calculations. The energies given throughout the paper are Gibbs free energy values *G* computed with Gaussian 03 at 298 K (entropy revise at the reaction temperature of 60 °C) and *P* = 1 atm.

Acknowledgment. This work was supported by National Natural Science Foundation of China, the Major Basic Research Development Program (2006CB806106), Chinese Academy of Sciences, Science and Technology Commission of Shanghai Municipality, and the Croucher Foundation of Hong Kong. W.Q.W. and Q.P. gratefully acknowledge the Croucher Foundation of Hong Kong for a studentship.

Supporting Information Available: Spectral data for **1a–c**, **2a**, **b**, **6**, **9b**, and **10b**; X-ray analysis data of [PdCl₂(**1a**)] and [PdCl₂(**2a**)] (cif file). The coordinates of calculated structures, the relative free energies (kcal/mol) of calculated complexes and transition states in the C=C double bond rotating from the perpendicular conformation in **CP2** to coplanar conformation and optimized energies (hartree) from B3LYP calculations. Complete refs 6b and 19. This material is available free of charge via the Internet at <http://pubs.acs.org>.

JA7104174